

Influence of new reaction rates on ^{18}F production in novae

Alain Coc¹, Margarita Hernanz², Jordi José^{2,3}, and Jean-Pierre Thibaud¹

¹ Centre de Spectrométrie Nucléaire et de Spectrométrie de Masse, IN2P3-CNRS and Université Paris Sud, Bâtiment 104, 91405 Orsay Campus, France

² Institut d'Estudis Espacials de Catalunya/CSIC, Edifici Nexus-201, C/Gran Capità 2-4, E-08034 Barcelona, Spain

³ Departament de Física i Enginyeria Nuclear (UPC), Avinguda Víctor Balaguer, s/n, E-08800 Vilanova i la Geltrú (Barcelona), Spain

Received 28 January 2000 / Accepted 9 March 2000

Abstract. Gamma-ray emission from classical novae is dominated, during the first hours, by positron annihilation resulting from the beta decay of radioactive nuclei. The main contribution comes from the decay of ^{18}F and hence is directly related to ^{18}F formation during the outburst. A good knowledge of the nuclear reaction rates of production and destruction of ^{18}F is required to study ^{18}F synthesis in novae and the resulting gamma-ray emission. The rates relevant for the main mode of ^{18}F destruction (i.e. through proton captures) have been the object of many recent experiments. However, subsequent analyses were focused on providing rates for X-ray burst nucleosynthesis not valid at nova temperatures (lower than 3.5×10^8 K). Accordingly, it is crucial to propose and discuss new reaction rates, incorporating all new experimental results, down to the domain of nova nucleosynthesis. We show that in this temperature regime, the $^{18}\text{F}(\text{p},\gamma)^{19}\text{Ne}$ and $^{18}\text{F}(\text{p},\alpha)^{15}\text{O}$ reaction rates remain uncertain and deserve further experimental and theoretical efforts. Our hydrodynamic calculations including the new nuclear rates demonstrate that their impact on ^{18}F synthesis in nova explosions is quite large and, consequently, the early gamma-ray emission from classical novae is also affected.

Key words: Nuclear reactions, nucleosynthesis, abundances – Novae, cataclysmic variables – Gamma rays: theory

1. Introduction

Classical novae emit gamma-ray radiation at and below 511 keV during the early epochs after the explosion. This emission is produced by electron-positron annihilation in the expanding envelope, and the subsequent Comptonization of the resulting gamma-ray photons, and it shows a line, at 511 keV, and a continuum, between 20 and 511 keV (Gómez-Gomar et al. 1998). The positrons responsible for this emission come mainly from the disintegration of ^{18}F (Leising & Clayton 1987; Gómez-Gomar et al. 1998), because its lifetime ($\tau=158$ min) is such that positrons are

emitted at the “right time”, i.e., when the expanding envelope starts to be transparent to gamma-ray radiation. Therefore, the amount of radiation emitted strongly depends on the ^{18}F content of the nova envelope.

The synthesis of ^{18}F in novae depends largely on some key nuclear reaction rates of ^{18}F destruction and production which are far from being well known. This is the case, in particular, of the $^{18}\text{F}(\text{p},\gamma)^{19}\text{Ne}$ and $^{18}\text{F}(\text{p},\alpha)^{15}\text{O}$ reactions. Recent experimental studies (Graulich et al. 1997; Utku et al. 1998) drastically improved the knowledge of these reaction rates with respect to previous studies (Wiescher & Kettner 1982). In a recent paper (Hernanz et al. 1999), we have analyzed the influence of these rates (Utku et al. 1998) of $^{18}\text{F}(\text{p},\gamma)^{19}\text{Ne}$ and $^{18}\text{F}(\text{p},\alpha)^{15}\text{O}$ on the final yields of ^{18}F for different models of CO and ONe novae. The effect of the new rates was important, since a factor of 10 reduction in the yields and in the resulting gamma-ray fluxes was obtained for all the models. Therefore, we concluded that a more detailed analysis of the reaction rates was necessary, in order to predict the gamma-ray emission of classical novae.

The rates proposed by Utku et al. (1998) were limited to relatively high resonance energies and temperature domains, more appropriate for temperatures typical of X-ray bursts than for those of classical novae. The reason is that for their determination neither the influence of uncertainties on low energy resonance strengths (based on assumed reduced width) nor the effect of *all* low energy resonance tails were considered. At higher temperatures the rates are more reliable since their main contributions come from two directly measured resonances. The purpose of this paper is to provide rates for the $^{18}\text{F}(\text{p},\gamma)^{19}\text{Ne}$ and $^{18}\text{F}(\text{p},\alpha)^{15}\text{O}$ reactions valid in the domain of temperature of nova nucleosynthesis, incorporating the latest experimental data. In addition to the nominal rate, we provide upper and lower limits. Since other nuclear reactions also affect ^{18}F synthesis in novae, a global analysis is done, including results from the recent NACRE compilation (Angulo et al. 1999). With the new rates affecting ^{18}F synthesis, new nova models have been computed, in

order to determine the mass of ^{18}F they eject and the impact of the new yields on their early gamma-ray emission.

The organisation of this paper is the following. In section 2 we describe the nucleosynthesis of ^{18}F . In section 3 we discuss in detail the $^{18}\text{F}+\text{p}$ rates and the corresponding uncertainties while in the following section (4), we briefly discuss other recently published rates. In section 5 we present new results that show the influence of these new rates on ^{18}F production. Following the conclusion, an appendix gives some analytical approximations to the rates.

2. Synthesis of ^{18}F in classical novae

In this Section, we will focus on the nuclear paths leading to ^{18}F synthesis, through a detailed analysis of a representative model of an ONe nova : a $1.25 M_{\odot}$ white dwarf, accreting solar-like matter at a rate of $2 \times 10^{-10} M_{\odot} \cdot \text{yr}^{-1}$, assuming a 50% degree of mixing with the outermost core of composition taken from Ritossa, García-Berro & Iben (1996) (mainly ^{16}O and ^{20}Ne with traces of other Ne, Na and Mg isotopes). The evolutionary sequences leading to a nova outburst have been computed with an updated version of the code SHIVA (see José & Hernanz 1998), a one-dimensional, implicit, hydrodynamical code in Lagrangian formulation, which follows the course of the explosion from the onset of accretion up to the expansion and ejection stages. The nuclear reaction network is described in José et al. (1999), and in Hernanz et al. (1999). In particular, we use the reaction rates for proton captures on ^{18}F and ^{17}O based on Utku et al. (1998) and Landré et al. (1989), respectively.

The synthesis of ^{18}F in nova outbursts takes place within the hot-CNO cycle (see fig. 1). Regardless of the nova type (either CO or ONe, according to the composition of the underlying white dwarf), the initial ^{16}O abundance is quite large (up to 25% by mass). Hence, initial ^{16}O is the main source of the formation of ^{18}F , either through the chain $^{16}\text{O}(\text{p},\gamma)^{17}\text{F}(\text{p},\gamma)^{18}\text{Ne}(\beta^+)^{18}\text{F}$ or through $^{16}\text{O}(\text{p},\gamma)^{17}\text{F}(\beta^+)^{17}\text{O}(\text{p},\gamma)^{18}\text{F}$, which reflects a competition between (p,γ) reactions and β^+ -decays.

Snapshots of the evolution of isotopes relevant to ^{18}F synthesis (i.e., $^{16,17}\text{O}$, $^{17,18,19}\text{F}$ and $^{18,19}\text{Ne}$) are shown in Fig. 2. At the early stages of the explosion, when the temperature achieved at the burning shell reaches $T_{bs} \simeq 5 \times 10^7$ K (Fig. 2, first panel), the main nuclear activity in this mass region is driven by $^{16}\text{O}(\text{p},\gamma)^{17}\text{F}$, followed by its β^+ -decay to ^{17}O . However, the temperature is not high enough to burn a significant fraction of ^{16}O . On the contrary, the abundance of ^{17}O rises by several orders of magnitude with respect to its initial content. Both $^{17,18}\text{F}$ are being synthesized at the burning shell by means of proton captures on $^{16,17}\text{O}$, respectively, whereas the amount of ^{19}F remains essentially unchanged. The minor activity driven by proton capture reactions onto $^{17,18}\text{F}$

results also in a moderate increase of both $^{18,19}\text{Ne}$ (below 10^{-10} by mass).

A similar trend is found when $T_{bs} \simeq 7 \times 10^7$ K (Fig. 2, second panel). The temperature rise increases the number of proton captures onto ^{16}O , leading to ^{17}F , which rapidly decays into ^{17}O . The effect of convection, which already extends through most of the envelope (i.e., ~ 150 km), is shown in the smooth distribution of both $^{17,18}\text{F}$, previously synthesized in the burning shell and efficiently carried away to the outer envelope. ^{19}F is in turn reduced down to 50% due to $^{19}\text{F}(\text{p},\alpha)^{16}\text{O}$, which dominates $^{19}\text{Ne}(\beta^+)^{19}\text{F}$.

When T_{bs} reaches 10^8 K (Fig. 2, third panel), ^{17}O shows a flat profile along the envelope, with a mean mass fraction of $\sim 3 \times 10^{-3}$, due to $^{16}\text{O}(\text{p},\gamma)^{17}\text{F}(\beta^+)^{17}\text{O}$, which dominates destruction through $^{17}\text{O}(\text{p},\gamma)^{18}\text{F}$. With respect to fluorine isotopes, we stress an important synthesis of $^{17,18}\text{F}$ at this stage, driven by $^{16}\text{O}(\text{p},\gamma)^{17}\text{F}$ and $^{17}\text{O}(\text{p},\gamma)^{18}\text{F}$, whereas ^{19}F is almost fully destroyed. $^{18,19}\text{Ne}$ continue to rise due to proton captures onto $^{17,18}\text{F}$.

A dramatic change is found as soon as the burning shell reaches 2×10^8 K (Fig. 2, fourth panel). At this time, the mass fraction of ^{16}O has been reduced down to $\sim 3 \times 10^{-2}$. For the first time, ^{17}O decreases (by one order of magnitude with respect to the amount shown in previous panel), since destruction through $^{17}\text{O}(\text{p},\gamma)^{18}\text{F}$ dominates $^{17}\text{F}(\beta^+)^{17}\text{O}$ in the vicinity of the burning shell. On the contrary, ^{17}F exhibits a significant rise, up to $\sim 3 \times 10^{-2}$ by mass (i.e., one order of magnitude higher than in previous panel), so that the amount of ^{17}F becomes larger than that of ^{17}O in almost all the envelope. Again, $^{16}\text{O}(\text{p},\gamma)^{17}\text{F}$ dominates both $^{17}\text{O}(\text{p},\gamma)^{18}\text{Ne}$ and $^{17}\text{F}(\beta^+)^{17}\text{O}$ near the burning shell. The evolution of ^{19}F is still dominated by $^{19}\text{F}(\text{p},\alpha)^{16}\text{O}$, which in fact has no significant influence on the ^{16}O content. Also noticeable is the dramatic rise of both $^{18,19}\text{Ne}$, which increase by several orders of magnitude, mainly due to the fact that at such temperatures, proton captures onto $^{17,18}\text{F}$ become faster than the corresponding β^+ -decays. It is worth noticing that at this stage, a non-negligible path leading to ^{18}F synthesis is now driven by $^{18}\text{Ne}(\beta^+)^{18}\text{F}$, basically at the outer envelope shells, which compensates an efficient destruction through proton captures near the burning shell.

The burning shell achieves a maximum temperature of 2.51×10^8 K (Fig. 2, fifth panel). ^{16}O is reduced to 0.096 by mass in the burning shell. Whereas ^{17}O is destroyed by (p,α) and (p,γ) reactions at the burning shell, its mean abundance in the envelope increases due to $^{17}\text{F}(\beta^+)^{17}\text{O}$ which dominates in almost all the envelope. On the contrary, ^{17}F is generated in the burning shell by means of $^{16}\text{O}(\text{p},\gamma)^{17}\text{F}$, whereas it is being destroyed by β^+ -decays in the outer envelope. The evolution of ^{18}F reflects a competition between destruction and creation modes at different locations of the envelope: whereas its content is reduced by both $^{18}\text{F}(\text{p},\alpha)^{15}\text{O}$ reactions at the burning shell and by $^{18}\text{F}(\beta^+)^{18}\text{O}$ at the outer envelope, a dominant source for

^{18}F synthesis through $^{17}\text{O}(\text{p},\gamma)^{18}\text{F}$ is found at the intermediate shells. Proton captures onto $^{17,18}\text{F}$ and convective transport continue to pump $^{18,19}\text{Ne}$ to the outer envelope shells, which is at the origin of the rise of ^{19}F at this stage (through $^{19}\text{Ne}(\beta^+)^{19}\text{F}$).

Shortly after, due to the sudden release of energy from the short-lived species ^{13}N , $^{14,15}\text{O}$ and ^{17}F , the envelope begins to expand. As a result of the drop in temperature, (p,γ) and (p,α) reactions are basically restricted to the vicinity of the burning shell, whereas most of the envelope is dominated by β^+ -decays (Fig. 2, sixth and seventh panels). Hence, whereas ^{17}O is powered by $^{17}\text{F}(\beta^+)^{17}\text{O}$ along the envelope, the amount of ^{17}F and $^{18,19}\text{Ne}$ decreases significantly. The ^{18}F abundance at these late-time stages of the outburst increases due to $^{17}\text{O}(\text{p},\gamma)^{18}\text{F}$, which is dominant at the intermediate layers of the envelope (whereas in the vicinity of the burning shell ^{18}F is efficiently destroyed by $^{18}\text{F}(\text{p},\alpha)^{15}\text{O}$, the outer envelope is dominated by $^{18}\text{F}(\beta^+)^{18}\text{O}$). Moreover, destruction of ^{19}F through $^{19}\text{F}(\text{p},\alpha)^{16}\text{O}$ at the burning shell is dominated by $^{19}\text{Ne}(\beta^+)^{19}\text{F}$ elsewhere.

The final stages of the outburst (Fig. 2, eighth panel), as the envelope expands and cools down, are dominated by the release of nuclear energy by β^+ -decays such as $^{18}\text{F}(\beta^+)^{18}\text{O}$, or $^{17}\text{F}(\beta^+)^{17}\text{O}$. The resulting mean abundance of ^{18}F in the ejected shells in this Model is $X(^{18}\text{F}) = 2.7 \times 10^{-4}$. Most of the envelope is, however, dominated by the large abundances of $^{16,17}\text{O}$ ($X(^{16}\text{O}) = 6.8 \times 10^{-2}$, $X(^{17}\text{O}) = 3.9 \times 10^{-2}$). A residual ^{17}F , which is still decaying into ^{17}O , and a non-negligible amount of ^{19}F (3×10^{-6} , by mass) are also present.

In summary, the synthesis of ^{18}F in classical novae is essentially controlled by five proton-capture reactions, $^{16}\text{O}(\text{p},\gamma)^{17}\text{F}$, $^{18}\text{F}(\text{p},\gamma)^{19}\text{Ne}$, $^{18}\text{F}(\text{p},\alpha)^{15}\text{O}$, $^{17}\text{O}(\text{p},\gamma)^{18}\text{F}$, $^{17}\text{O}(\text{p},\alpha)^{14}\text{N}$, and several β^+ -decays. Accordingly, the corresponding reaction rates deserve further attention and their uncertainties are discussed in Sect. 3 for the $^{18}\text{F}+\text{p}$ rates and Sect. 4 for the other rates.

3. The $^{18}\text{F}(\text{p},\alpha)^{15}\text{O}$ and $^{18}\text{F}(\text{p},\gamma)^{19}\text{Ne}$ reaction rates

Uncertainties on the $^{18}\text{F}(\text{p},\gamma)^{19}\text{Ne}$ and $^{18}\text{F}(\text{p},\alpha)^{15}\text{O}$ reaction rates used to reach many orders of magnitude due to the very limited spectroscopic data available for ^{19}Ne in the domain of interest. The rate estimated by Wiescher & Kettner (1982) has become obsolete by the recent measurements of Rehm et al. (1995), Coszach et al. (1995), Rehm et al. (1996, 1997) and in particular by the work of Graulich et al. (1997), Utku et al. (1998) and Butt et al. (1998). We concentrate on the faster $^{18}\text{F}(\text{p},\alpha)^{15}\text{O}$ reaction but most of the discussion also applies to the $^{18}\text{F}(\text{p},\gamma)^{19}\text{Ne}$ one.

Before 1997 and below the excitation energy (E_x) corresponding to the resonance energy (E_r) of 0.4 MeV, only two levels were known $E_x = 6.437$ and 6.742 MeV but

with unknown or uncertain spins and parity (J^π)¹. On the contrary, various levels were known in the corresponding region of ^{19}F , the conjugate nucleus (see Fig. 3). For instance, in the $E_r=0.-1.$ MeV region, only 6 levels were known and many spins unknown in ^{19}Ne , while 19 levels had been observed in the corresponding ^{19}F region. Hence, for the estimation of the rates, Wiescher & Kettner (1982) considered three known levels at $E_x = 6.437$, 6.742 and 6.862 MeV and postulated three others. The corresponding rate was highly uncertain since the location of these three postulated levels was approximate and because other levels found in ^{19}F are expected to have counterparts in ^{19}Ne in the region of interest. This is the case, in particular, of the $E_x, J^\pi = 6.429, 1/2^-$, $6.497, 3/2^+$ and $6.527, 3/2^+$ levels of ^{19}F corresponding to strong expected resonances because of their low centrifugal barrier, i.e. low transferred orbital angular momentum (ℓ_p) of 1, 0 and 0 respectively.

Even though the recent experiments have not been able to find all the counterparts of the ^{19}F levels (see Fig. 3), they provided direct measurement for the strengths of two resonances which likely dominate the rate in the domain of nova nucleosynthesis and the location of several new ^{19}Ne levels. The strength of the resonance corresponding to the $E_x = 6.742$ MeV level ($E_r=330$ keV) has recently been measured directly by Graulich et al. (1997) with a ^{18}F beam provided by the Louvain-La-Neuve facility. This level is thought to be the analog of the $6.787, 3/2^-$ ^{19}F level. The measured strength ($\omega\gamma$), 3.5 ± 1.6 eV (Graulich et al. 1997), is in good agreement with the Wiescher & Kettner (1982) estimate and accordingly does not induce a significant change in the rate. On the contrary, the resonance associated with the $E_x, J^\pi = 7.067$ MeV, $3/2^+$ level ($E_r=659$ keV) strongly modifies the rates. It has been studied by Rehm et al. (1995, 1996), Coszach et al. (1995), Graulich et al. (1997), Utku et al. (1998) and Butt et al. (1998) and its strength has been measured directly (Coszach et al. 1995; Graulich et al. 1997). It is located well outside of the Gamow peak but due to its total width ($\Gamma \approx 30$ keV), the contribution of its tail alone is greater than the Wiescher & Kettner (1982) rate in the domain of nova nucleosynthesis. However, no counterpart of this broad level was known in ^{19}F . The closest $3/2^+$ ^{19}F level is located at $E_x = 7.262$ but its width is much smaller ($\Gamma < 6$ keV). To remove this incompatibility, Rehm et al. (1996) claimed that the 7.067 MeV width could be smaller ($\Gamma \approx 14$ keV). A $7.114, 7/2^+$ level was known in ^{19}F with the possibility that it hides an unresolved $J^\pi = 3/2^+$ level as suggested by Smotrich et al. (1961). A recent gamma ray spectroscopy study (Butt et al. 1998) of ^{19}F produced by the $^{15}\text{N}(\alpha,\gamma)^{19}\text{F}$ reaction has confirmed the presence of a 7.101 MeV, $3/2^+$, $\Gamma = 28 \pm 1$ keV level.

¹ For more detailed explanations of the standard nuclear physics notations used, see e.g. the appendix in José et al. (1999).

Hence the high width found by Coszach et al. (1995) and Utku et al. (1998) for the $E_x, J^\pi = 7.067 \text{ MeV}, 3/2^+, ^{19}\text{Ne}$ level can be understood. (Note however that this analog assignment has been questioned very recently by Fortune & Sherr (2000).)

Utku et al. (1998) have also found three new ^{19}Ne levels and have made tentative assignments of analog levels in ^{19}F (see Fig.3). They recognized the 6.437 MeV, $1/2^-$ level ($E_r=26 \text{ keV}$) as the analog of the 6.429, $1/2^-$, $\Gamma = 280 \text{ keV}$ one in ^{19}F from its large measured width ($216 \pm 19 \text{ keV}$). Even though it is located at a very low energy (in the context of novae) it is so broad that its tail may lead to a significant contribution to the rate (see Fig.4). The 6.449 MeV $3/2^+$ ($E_r=38 \text{ keV}$) level is one of the three new ones found by Utku et al. (1998). It is also of great importance since the contribution of its tail can dominate the astrophysical factor in the relevant energy range (see Fig.4). In comparison the two other new levels give a smaller (6.698 MeV $5/2^+$, $E_r=287 \text{ keV}$) or negligible contribution (6.419 MeV $3/2^+$, $E_r=8 \text{ keV}$).

A new rate has been provided by Utku et al. (1998), using their new data together with available spectroscopic information on ^{19}Ne and ^{19}F supplemented by estimates of radiative and proton widths when missing. This rate is already higher by a factor of up to $\approx 3 \times 10^2$ when compared with Wiescher & Kettner (1982). Nevertheless, even though this rate is now set on a firmer basis than the Wiescher & Kettner (1982) one, it remains quite uncertain as it depends directly on the estimated proton widths. Except for the two resonances whose strengths have been measured directly by Graulich et al. (1997), the proton widths are assumed to be equal to 0.1 or 0.01 Wigner limit, i.e. $\theta_p^2=0.1$ or 0.01, according to their parity (Utku et al. 1998). For the resonances considered here, one has $\Gamma_p \ll \Gamma_{Tot} \approx \Gamma_\alpha$ so that their strengths are ($\omega\gamma \approx \omega\Gamma_p$) proportional to chosen θ_p^2 values. Accordingly, to obtain lower and upper limits for the rate, we used the two extreme cases $\theta_p^2=0$ and $\theta_p^2=1$ respectively and regardless of parity but kept Utku et al. (1998) θ_p^2 values for the nominal rate (see Fig.6). The lower limit is quite certain as it is given by the contribution of the two directly measured resonances whose parameters are now reliably determined. It remains higher than the Wiescher & Kettner (1982) rate above $\approx 50 \times 10^6 \text{ K}$. The nominal rate is conditioned by the rather arbitrary choice of $\theta_p^2=0.1$ or 0.01 that we adopt following Utku et al. (1998). However, our nominal rate is significantly higher [up to a factor of ≈ 10 and 30 around 10^8 K for (p, α) and (p, γ) reactions] than the one from Utku et al. (1998) for typical nova temperatures (see Fig.6). This is due to the inclusion of the contribution of the tail ($\Gamma_{Tot} = \Gamma_\alpha = 4.3 \text{ keV}$) of the 6.449 MeV level (see Fig. 4) not considered by Utku et al. (1998). The corresponding rates (p, α) are presented in Fig.6 and have been calculated by numerical integration of the Breit-Wigner formula for all broad resonances. For the (p, γ) rates, we used the same procedure to obtain the low, nominal and

high rates (see Figs. 5 and 7). Radiative widths were taken from ^{19}F analog levels as in Utku et al. (1998) except for the important resonance at 659 keV as Bardayan et al. (1999) provided an experimental value ($\Gamma_\gamma=0.39 \text{ eV}$) for the analog level. We also adopted the direct capture (DC) contribution from Utku et al. (1998) even though the spectroscopic factors used ($^{18}\text{O} \otimes p$ instead of $^{18}\text{F} \otimes p$ or even $^{18}\text{F} \otimes n$) may not be the more appropriate. These rates have been calculated using all the available spectroscopic data collected in Table II of Utku et al. (1998) except for the inclusion of a new gamma width for the 659 keV resonance and for a different proton width for the 26 keV resonance [1% of the Wigner limits i.e. $2.5 \times 10^{-17} \text{ eV}$, as for other negative parity resonances, instead of $6.6 \times 10^{-20} \text{ eV}$ of unknown origin in Utku et al. (1998)]. These numbers are taken at face value to calculate the nominal rate only. For the low and high rates unknown proton widths are allowed to vary between 0 and the Wigner limit as discussed above. It is clear that this range ($0 < \theta_p^2 < 1$) represents the most extreme values as are the corresponding rates. This should be kept in mind when interpreting the astrophysical implications.

However a few points have been neglected due to the lack of experimental or theoretical information. First of all, the identification of all $E_x \lesssim 6.6 \text{ MeV}$ analog levels is not complete yet (see Fig. 3) and is not certain. In particular, new contributions to the nominal and high rates corresponding to missing levels cannot be ruled out. The tail of the 38 keV resonance has been calculated using the large total width derived from the ^{19}F analog level proposed by Utku et al. (1998). Another $3/2^+$ level, with smaller width, lies 30 keV below in ^{19}F . It has been assigned (Utku et al. 1998) to be the analog level corresponding to the 8 keV ($E_x=6.419 \text{ MeV}$) resonance in $^{18}\text{F}+p$ (see Fig. 3). It is possible that the analog assignment for these two levels is inversed or that they are mixed but at least one or the other resonance (8 or 38 keV) should be broad enough to dominate the rates at low nova temperature. For the (p, γ) rates, we neglected any difference of radiative widths between analog levels and the uncertainty on the DC contribution in front of the uncertainty on the proton widths. These rates do not either include possible interference effects arising from the interference between the $3/2^+$ resonances located at 38 and 659 keV. In a favourable case (when $\theta_p^2 \approx 0.01$ for the 38 keV resonance), destructive interference could reduce the low rate by a factor of ≈ 10 in the sensitive $T \approx 10^8 \text{ K}$ region. However, at present the rates provided in the appendix are those we recommend.

4. Other reactions affecting ^{18}F production

According to the recent compilation of charged-particle induced thermonuclear reaction rates NACRE (Angulo et al. 1999), the rate for $^{16}\text{O}(p,\gamma)^{17}\text{F}$ is rather well known and suffers from a little uncertainty (i.e., a factor of ~ 2 between the high and low rates). Even

though ^{17}F has a much shorter lifetime than ^{18}F , its destruction by proton capture is rather well known at nova temperatures and should not affect the analysis of Sect. 2. Below $\approx 4 \times 10^8$ K, the $^{17}\text{F}(p,\gamma)^{18}\text{Ne}$ reaction rate is dominated by the effect of direct capture on bound ^{18}Ne levels. This contribution is expected to suffer little uncertainty since it has been calculated (Wiescher & Kettner 1982; García et al. 1991) using experimental neutron spectroscopic factors from the mirror nucleus ^{18}O . The lowest resonances are located at $E_r = 0.586, 0.655$ and 0.600 MeV (Bardayan et al. 1999) too high to contribute, even by their tails, to the rate below $\approx 4 \times 10^8$ K. Partial widths are reasonably known through experiments, shell model calculations or from the conjugate levels (Wiescher & Kettner 1982; García et al. 1991) and are such that $\Gamma_p \gg \Gamma_\gamma$ (i.e. $\omega\gamma = \omega\Gamma_\gamma$). A long standing uncertainty (Wiescher & Kettner 1982; Wiescher, Görres & Thielemann 1988; García et al. 1991) concerned the location of the $\ell=0$, 0.600 MeV resonance associated with the 4.524 MeV, 3^+ level. Fortunately, the resonance energy first measured by García et al. (1991), has been experimentally confirmed very recently by Bardayan et al. (1999). Hence the uncertainty associated with the $^{17}\text{F}(p,\gamma)^{18}\text{Ne}$ rate appears negligible within the domain of nova nucleosynthesis.

According to NACRE (Angulo et al. 1999), the $^{17}\text{O}(p,\alpha)^{14}\text{N}$ (Fig. 8) and $^{17}\text{O}(p,\gamma)^{18}\text{F}$ (Fig. 9) reaction rates present large uncertainties at temperatures below a few 10^8 K. The increase in the rates around 50×10^6 (Angulo et al. 1999) is due to the contribution of a $E_r = 66$ keV resonance (Landré et al. 1989; Blackmon et al. 1995), not included in Caughlan & Fowler (1988). The large uncertainty around 2×10^8 K (Angulo et al. 1999), well within the range of temperature reached in nova outbursts, is due to the unknown contribution of a 179.5 keV resonance associated with the $E_x = 5786$ keV (^{18}F) level. The upper limits for the strengths $[(p,\gamma)$ and $(p,\alpha)]$ of this resonance are calculated (Angulo et al. 1999) from the partial widths extracted by Rolfs, Berka & Azuma (1973) and the upper limit for the proton width from Landré et al. (1989). As usual, for the calculation of the contribution of this resonance to the NACRE low, recommended and high rates, its strength has been taken equal to 0, 10% and 100% of the experimental upper limit. Accordingly, the NACRE recommended rate is somewhat arbitrary in the temperature domain affected by the 179.5 keV resonance (Figs. 8 and Figs. 9)

5. Results: effect of new rates on ^{18}F synthesis

New models of a $1.25 M_\odot$ ONe nova have been computed with the SHIVA code, in order to analyze the effect of the new nuclear reaction rates. For the $^{18}\text{F}+p$ rates, we have adopted the low, high and nominal prescriptions described in section 3, whereas for the $^{17}\text{O}+p$

ones we have adopted the NACRE rates (see Table 1). It is important to stress that the energetics of the explosion remains practically unchanged with the new $^{18}\text{F}+p$ and $^{17}\text{O}+p$ reaction rates, since these reactions are not the ones affecting most the evolution (see José & Hernanz (1998) and José et al. (1999) for a deep analysis of the reaction rates which have the largest influence in nova explosions). Therefore, the maximum temperature attained in the burning shell at the base of the accreted envelope, $T_{max} = 2.51 \times 10^8$ K, the mean kinetic energy and the ejected mass, $\Delta M_{ejec} = 1.8 \times 10^{-5} M_\odot$, are unchanged with respect to previous models (i.e., José et al. (1999)).

Two previously computed evolutionary sequences, with the same white dwarf mass and composition, are adopted as *old* models for the purpose of comparison: a case with Wiescher & Kettner (1982) rates (see José & Hernanz (1998) for the yields and Gómez-Gomar et al. (1998) for the γ -ray spectra) and a case with Utku et al. (1998) rates (see Hernanz et al. (1999) for the yields and the spectra). In both of them, the Caughlan & Fowler (1988) updated by Landré et al. (1989) rates for $^{17}\text{O}+p$ were adopted. In Table 1 we show the ^{18}F yields obtained with the new rates, as well as those with the *old* models. We see that yields with the nominal $^{18}\text{F}+p$ rates are smaller by a factor of 30 than those with the older rates, as expected. In fact, the reduction in ^{18}F production is even larger (by a factor of 3) than the one obtained with Utku et al. (1998) rates (see Hernanz et al. (1999)), as a consequence of the inclusion of the tail of the resonance at 38 keV (see section 3).

Concerning the effect of the new $^{17}\text{O}+p$ rates, a reduction by an extra factor of 2 is obtained when the NACRE recommended rates, instead of the old Caughlan & Fowler (1988) and Landré et al. (1989) ones, are adopted (together with $^{18}\text{F}+p$ nominal rates; see Table 1). In summary, our nominal yield of ^{18}F is 4.84×10^{-5} , which is 60 times smaller than the yield with the old Wiescher & Kettner (1982) rates (José & Hernanz 1998; Gómez-Gomar et al. 1998) and 6 times smaller than that with Utku et al. (1998) rates (Hernanz et al. 1999). The consequences of the reduced ^{18}F yields are quite large for the early gamma-ray output, which is directly related to the amount of ^{18}F synthesized. The reduced content of ^{18}F in an expanding envelope with similar physical and dynamical properties, translates directly into a reduced positron annihilation gamma-ray flux, roughly by the same factor as the ^{18}F decrease. This was shown in Hernanz et al. (1999), where complete computations of the gamma-ray spectra were performed with the ^{18}F yields obtained with Utku et al. (1998) rates, for different masses and compositions of the white dwarf. With the rates presented here, the reduction of the predicted fluxes becomes larger by a factor of 6, for the combined nominal $^{18}\text{F}+p$ and recommended $^{17}\text{O}+p$ rates. In summary, if we compare with results in Gómez-Gomar et al. (1998), where ^{18}F yields were computed with Wiescher & Kettner (1982), the

511 keV and continuum fluxes for a $1.25 M_{\odot}$ ONe nova should be reduced by a factor of 60.

Another important point to stress is the impact of the uncertainty in the rates on the computed yields. The above *nominal* yields rely upon *recommended* or *nominal* rates which contain assumed values ($\theta_p^2=0.01$ or 0.1 for $^{18}\text{F}+p$ and 10% of an experimental upper limit for $^{17}\text{O}+p$). Hence, the nominal yield should not be dissociated from the large remaining uncertainties. From our results (see Table 1) we conclude that the range between high and low prescriptions for the $^{18}\text{F}+p$ rates translates into an uncertainty (maximum versus minimum yield ratio) of a factor of 310, a quite large value, whereas for the $^{17}\text{O}+p$ rates the uncertainty is a factor of 10. (It is worth noticing that the results obtained with the Utku et al. (1998) rates fall within the limits obtained with the new rates; see Table 1). The corresponding uncertainties in the gamma-ray fluxes are of the same order of magnitude. This points out the interest of more accurate determinations of the $^{18}\text{F}+p$ and $^{17}\text{O}+p$ rates.

6. Conclusions

We have investigated the ^{18}F formation and destruction in nova outbursts, identified the key reactions (proton capture on ^{18}F and ^{17}O) and analysed their rates. The proton capture rates on ^{18}F are higher than the Wiescher & Kettner (1982) ones at nova temperatures due to the contribution of the tail of the 659 keV resonance whose large measured width (Coszach et al. 1995; Graulich et al. 1997) has been indirectly confirmed (Butt et al. 1998). Another important contribution comes from the tail of the 38 keV resonance which was neglected in previous studies. Its *nominal* contribution is larger than the 659 keV one but is proportional to its *assumed* reduced proton width θ_p^2 . The strengths (proton widths) of the low lying resonances are unknown and induce large uncertainties (factors of 100 to 1000) in the rates at nova temperatures. We have provided updated nominal rates for the two capture reactions together with upper and lower limits. The $^{17}\text{O}+p$ rates also display some large uncertainties at nova temperatures according to the recent compilation of Angulo et al. (1999).

We have used these new nuclear physics results in a fully hydrodynamical nova code to calculate the ^{18}F yields in novae for different rates : our low, nominal and high $^{18}\text{F}+p$ rates, and the low, recommended and high $^{17}\text{O}+p$ rates from Angulo et al. (1999). These results have been compared with models computed with the old Wiescher & Kettner (1982) rates (José & Hernanz 1998), and with more recent models with the Utku et al. (1998) rates (Hernanz et al. 1999). Two important results have been obtained. First, there is always a reduction of the amount of ^{18}F synthesized in a nova explosion, with the nominal rates for the $^{18}\text{F}+p$ reactions both alone and combined with the recommended rates for the $^{17}\text{O}+p$ reactions. The nominal ^{18}F yield (nominal $^{18}\text{F}+p$ and recommended for

$^{17}\text{O}+p$) is 4.84×10^{-5} by mass, which is 60 times smaller than the one obtained with Wiescher & Kettner (1982) rates and 6 times smaller than the one with Utku et al. (1998) rates (and Caughlan & Fowler (1988) and Landré et al. (1989) for $^{17}\text{O}+p$). The impact on the early gamma-ray spectrum of the nova is a reduction of the flux by the same amount (with respect to Gómez-Gomar et al. (1998) and Hernanz et al. (1999), respectively). Second, the yields are found to be very sensitive to the rates with resulting combined ($^{18}\text{F}+p$ and $^{17}\text{O}+p$) uncertainties of more than three orders of magnitude. This supports the need of new experimental and theoretical studies to improve the knowledge of the $^{18}\text{F}+p$ and $^{17}\text{O}+p$ rates and, consequently, allow for a larger reliability of the predictions of annihilation gamma-ray fluxes from novae, to be observed by current and future instruments.

Acknowledgements. This work was partially supported by PICS 319, PB98-1183-C02, PB98-1183-C03 and ESP98-1348.

References

- Angulo C., Arnould M., Rayet M., et al., (The NACRE collaboration) 1999, Nucl. Phys. A656, 3
- Bardayan D.W., Blackmon J.C., Brune C.R., et al., 1999, Phys. Rev. Lett. 83, 45
- Blackmon J.C., Champagne A.E., Hofstee M.A., et al., 1995, Phys. Rev. Lett. 74, 2642
- Butt Y.M., Hammer J.W., Jaeger M., et al., 1998, Phys. Rev. C58, R10
- Caughlan, G.R. Fowler, W.A., 1988, At. Data Nucl. Data Tables, 40, 283
- Coszach R., Cogneau M., Bain C.R., et al., 1995, Phys. Lett. B353, 184
- Fortune H.T. and Sherr R. 2000, Phys. Rev. C61, 024313-1
- García A., Adelberger E.G., Magnus P.V., et al., 1991, Phys. Rev. C43, 2012
- Gómez-Gomar J., Hernanz M., José J., Isern J., 1998, MNRAS 296, 913
- Graulich J.S., Binon F., Bradfield-Smith W., et al., 1997, Nucl. Phys. A626, 751
- Hahn K.I., Garcia A., Adelberger E.G., et al., 1996, Phys. Rev. C54, 1999
- Hernanz M., José J., Coc A., Gómez-Gomar J. Isern J., 1999, ApJ 526, L97
- José J., Coc A., Hernanz M. 1999, ApJ , 520, 347
- José J., Hernanz M. 1998, ApJ 494, 680
- Landré V., Aguer P., Bogaert G., et al., 1989, Phys. Rev. C40, 1972
- Leising M.D., Clayton D.D., 1987, ApJ 323, L57
- Park S.H., Kubono S., Hahn K.I., et al., 1999, Phys. Rev. C59, 1182
- Rehm K.E., Paul M., Roberts A.D., et al., 1995, Phys. Rev. C52, R460
- Rehm K.E., Paul M., Roberts A.D., et al., 1996, Phys. Rev. C55, 1950
- Rehm K.E., Jiang C.L., Paul M., et al., 1997, Phys. Rev. C53, R566
- Rolls C. Berka I., Azuma R.E., 1973, Nucl. Phys. A199, 306
- Ritossa C, García-Berro E., Iben I., 1996, ApJ 460, 489

- Smotrich H., Jones K.W., McDermott L.C., Benenson R.E.,
1961, Phys. Rev. 122, 232
- Tilley D.R., Weller H.R., Cheves C.M. Chasteler R.M., 1995,
Nucl. Phys. A595, 1
- Utku S., Ross J.G., Bateman N.P.T., et al., 1998, Phys. Rev.
C57, 2731 and C58, 1354
- Wiescher M., Görres J., Thielemann F.K., 1988, ApJ 326, 384
- Wiescher M. Kettner K.U. 1982, ApJ 263, 891

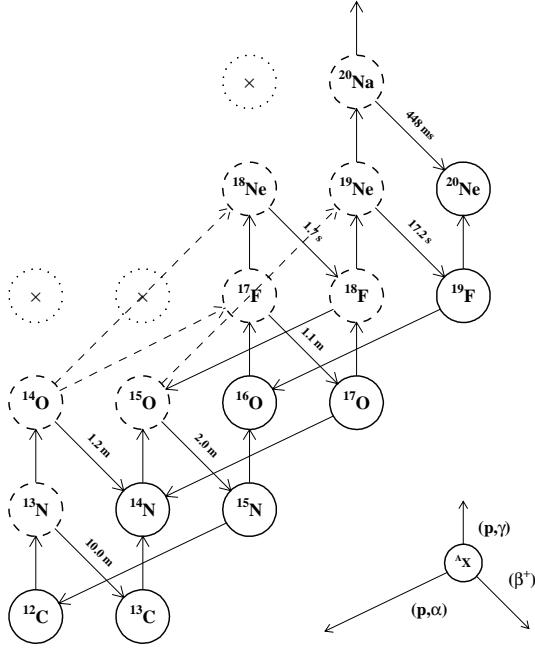


Fig. 1. Hot CNO cycle. Dashed and dotted circles represent beta unstable and proton unbound nuclei respectively. Dashed arrows represent reactions of negligible influence in novae.

Appendix: Updated rates

We give here the tabulated reaction rates for proton capture on ^{18}F resulting from numerical integrations (see § 3 and Figs. 6 and 7). For convenience, we also provide here formulas that approximate the nominal rates (As usual, T9 is the temperature in GK, $T9XY = T9 \cdot (X/Y)$ and $T9LN = \text{LOG}(T9)$ in FORTRAN notations.)

The following $^{18}\text{F}(p,\alpha)^{15}\text{O}$ nominal rate formula includes the contribution of the two measured resonances (330 and 659 keV) with additional contributions from the possible resonances at 38 keV, (with high energy tail) and 287 keV.

$$\begin{aligned} \text{SVD}_{\text{Dir}} = & 9.13\text{e}10/T923 \cdot \text{EXP}(-18.052/T913 - 0.672 \cdot T92) \cdot (1. + ! \text{ Tail} \\ & \& 0.0231 \cdot T913 + 6.12 \cdot T923 + 0.988 \cdot T9 + 9.92 \cdot T943 + 4.07 \cdot T953) ! 659 \text{ keV} \\ & \& + 5.78\text{e}5/T932 \cdot \text{EXP}(-3.830/T9) + 9.91\text{e}8/T932 \cdot \text{EXP}(-7.648/T9) + ! 330, 659 \text{ keV} \\ & \& 2.81\text{e}-6/T932 \cdot \text{EXP}(-0.441/T9) + 2706. \cdot \text{EXP}(3.8319 \cdot T9LN - 1.3450 \cdot ! 38 \text{ keV} \\ & \& T9LN \cdot \cdot 2 - .0001/T9 \cdot \cdot 3) + 4.46\text{e}4/T932 \cdot \text{EXP}(-3.331/T9) ! 287 \text{ keV} \end{aligned}$$

The following $^{18}\text{F}(p,\gamma)^{19}\text{Ne}$ nominal rate formula contains contributions from direct capture and from the 38, 287, 330 and 659 keV resonances.

$$\begin{aligned} \text{SVD}_{\text{Dir}} = & 3.98\text{e}7/T923 \cdot \text{EXP}(-18.052/T913) \cdot ! \text{ DC} \\ & \& (1. + 0.0231 \cdot T913 + 0.0885 \cdot T923 + 0.0143 \cdot T9) + \\ & \& 1.34\text{e}3/T932 \cdot \text{EXP}(-3.830/T9) + 1.51\text{e}4/T932 \cdot \text{EXP}(-7.648/T9) \\ & \& + \text{EXP}(-0.56781 + 3.6850 \cdot T9LN - 1.3636 \cdot T9LN \cdot \cdot 2 - .0001/T9 \cdot \cdot 3) \\ & \& + 8.26\text{e}-10/T932 \cdot \text{EXP}(-0.441/T9) + 12.2/T932 \cdot \text{EXP}(-3.331/T9) \end{aligned}$$

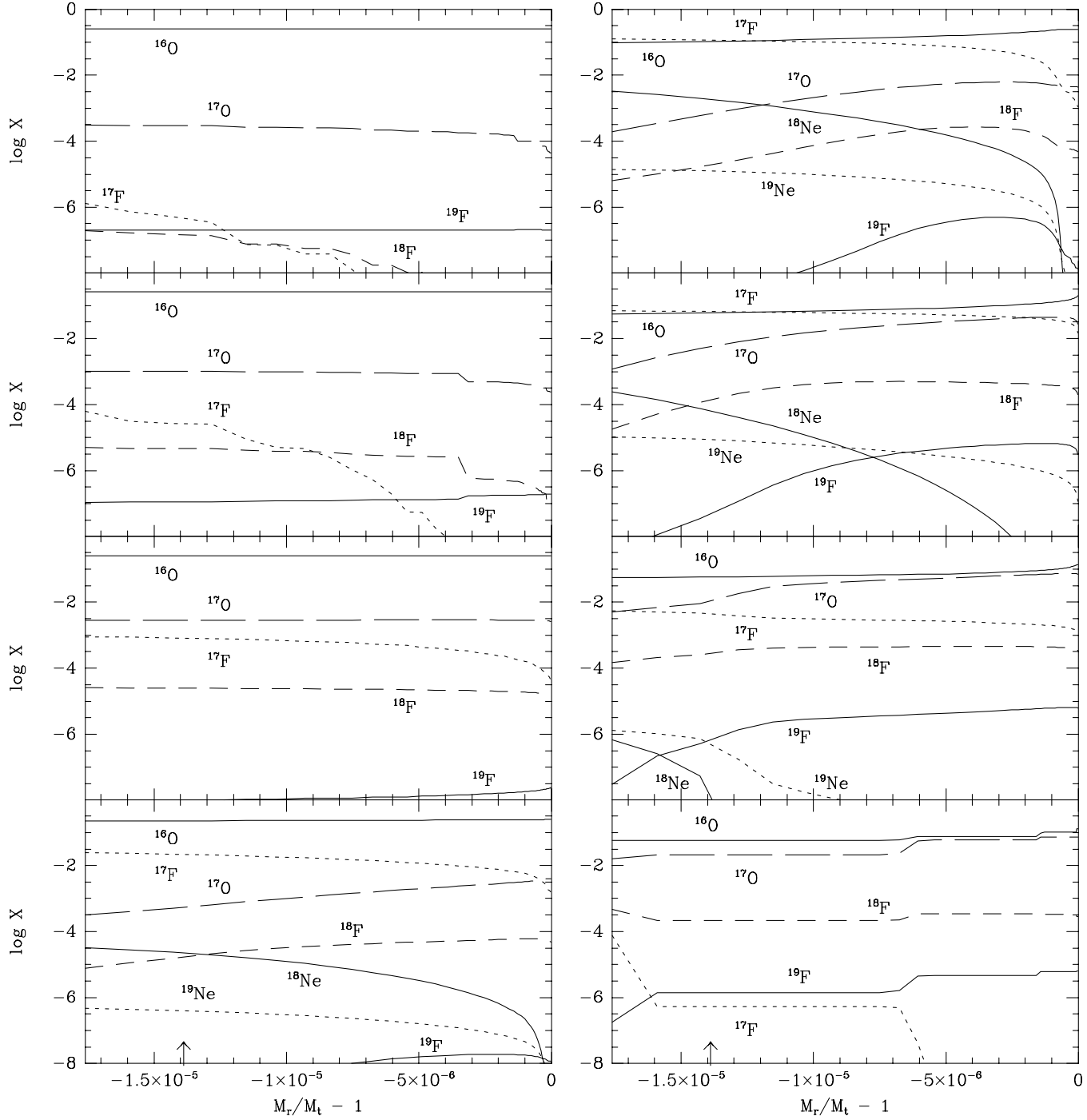


Fig. 2. Mass fractions of isotopes in the expanding envelope at various stages of the outburst. The horizontal axis corresponds to a relative mass coordinate where the origin is set at the surface of the envelope and where the arrow shows the limit of the ejected material. The panels are numbered from top to bottom and from left to right and correspond to temperatures of approximately 5×10^7 K, 7×10^7 K, 10^8 K, 2×10^8 K, $T_{\max} = 2.5 \times 10^8$ K, and to the last phases of the evolution, when the nova envelope has already expanded to a size of $R_{\text{vd}} \sim 10^9, 10^{10}$ and 10^{12} cm, respectively.

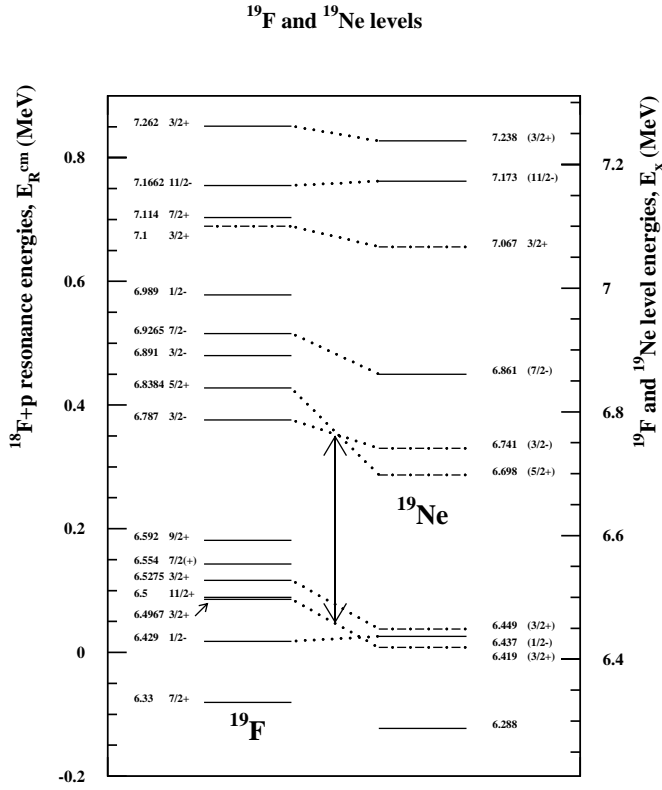


Fig. 3. Level scheme for ^{19}F and ^{19}Ne . Dotted lines relate conjugate levels suggested by Utku et al. 1998. The arrow represents the energy range where the presence of resonances (or tails of resonances) affects the reaction rates in the domain of temperature corresponding to nova outbursts. The dash-dotted lines represents new experimental data since Wiescher & Kettner (1982).

Table 1. Yields (in mass fraction) of ^{18}F 1 hour after T_{max} , for a $1.25 M_{\odot}$ ONe nova, for different prescriptions for the $^{18}\text{F}+p$ and $^{17}\text{O}+p$ nuclear reaction rates.

Rates for $^{18}\text{F}+p$	Rates for $^{17}\text{O}+p$	Reference	^{18}F
WK82	CF88+Lan89	JH98	2.80×10^{-3}
Utku98	CF88+Lan89	HJC99	2.50×10^{-4}
Low	CF88+Lan89	This work	8.19×10^{-4}
Nominal	CF88+Lan89	This work	9.78×10^{-5}
High	CF88+Lan89	This work	2.98×10^{-6}
Nominal	NACRE low	This work	1.58×10^{-5}
Nominal	NACRE rec.	This work	4.84×10^{-5}
Nominal	NACRE high	This work	1.67×10^{-4}

References for the rates: WK82 (Wiescher & Kettner 1982), CF88 (Caughlan & Fowler 1988), Lan89 (Landré et al. 1989), NACRE (Angulo et al. 1999). References for the models: JH98 (José & Hernanz 1998), HJC99 (Hernanz et al. 1999).

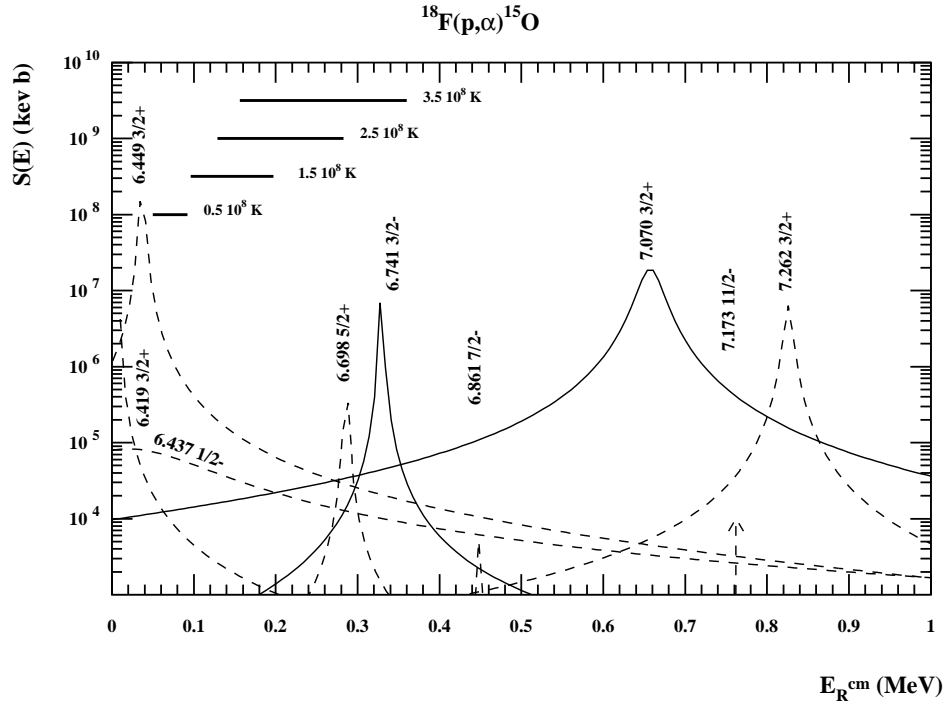


Fig. 4. Astrophysical S-factor for the $^{18}\text{F}(\text{p},\alpha)^{15}\text{O}$ reaction. The solid lines represent contributions from resonances whose strengths have been directly measured. Dashed curves represent assumed contributions from resonances corresponding to known ^{19}Ne levels. Possible contributions associated to expected levels in ^{19}Ne are not shown. Note the importance of the tail of the $E_r=38$ keV ($E_x=6.449$ MeV, $3/2^+$) resonance not considered in Utku et al. (1998).

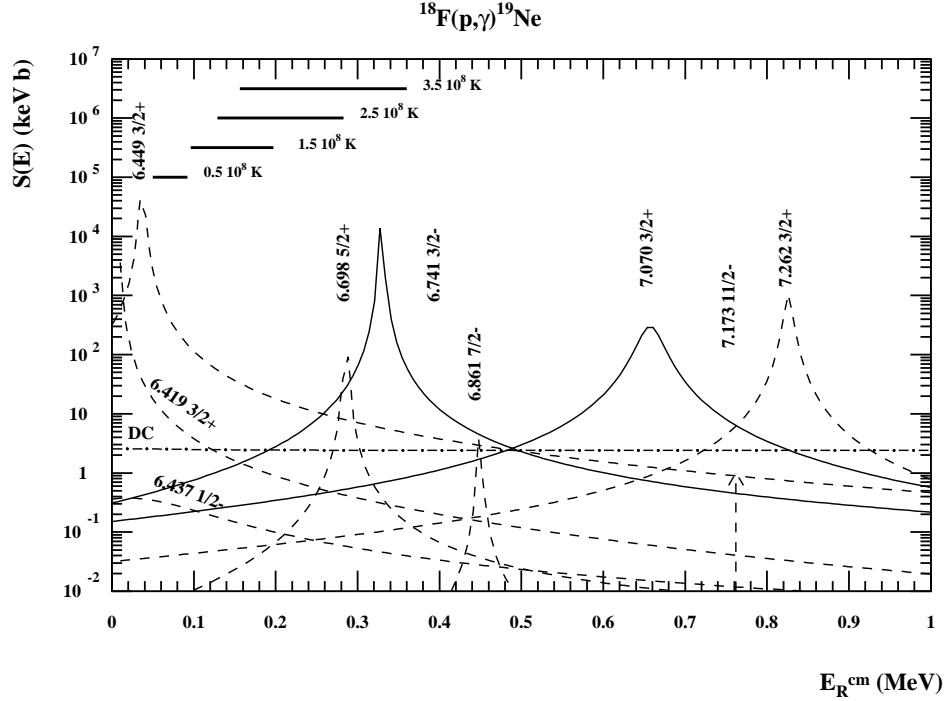


Fig. 5. Same as Fig. 4 but for the $^{18}\text{F}(\text{p},\gamma)^{19}\text{Ne}$ reaction.

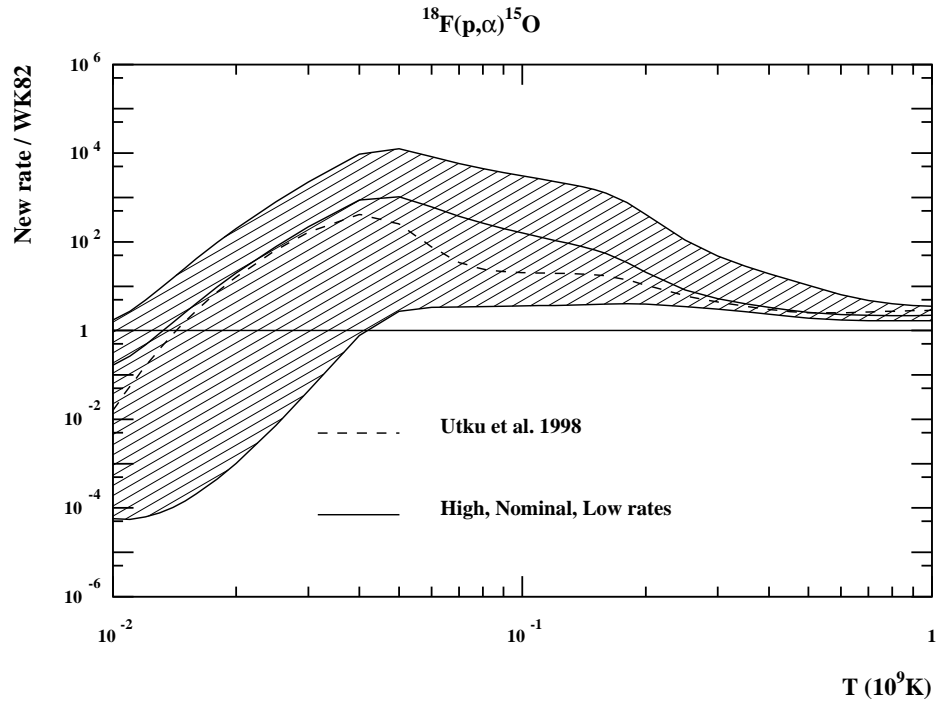


Fig. 6. $^{18}\text{F}(\text{p},\alpha)^{15}\text{O}$ rates compared to WK82. The solid lines represent the low, nominal and high rates and the hatched area the nuclear uncertainty. The dashed line represents the Utku et al. 1998 rate. All rates have been normalized to the WK82 one.

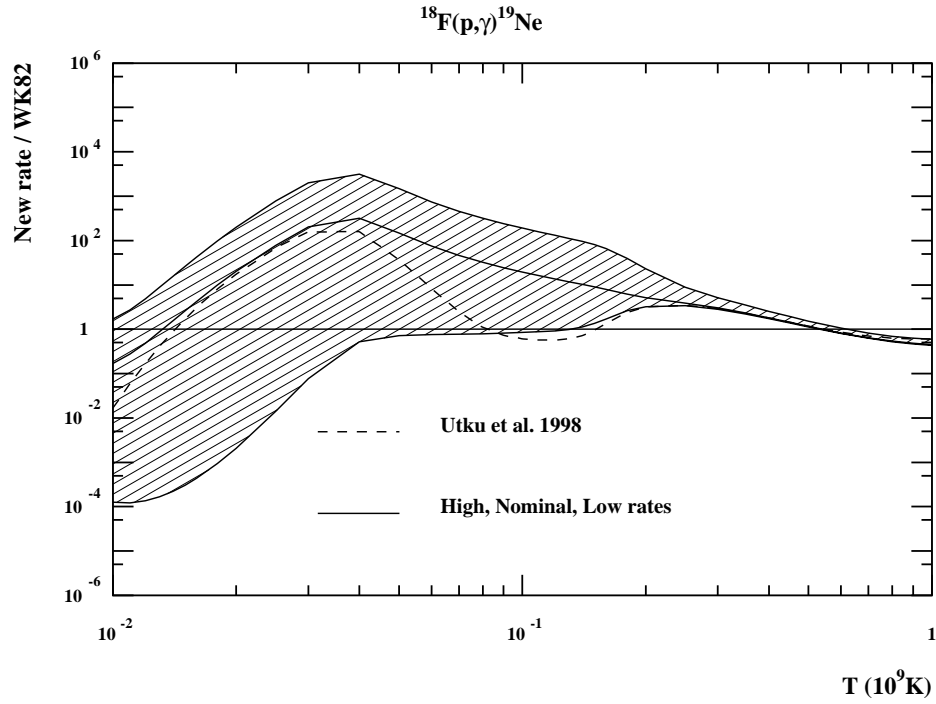


Fig. 7. Same as Fig. 6 but for the $^{18}\text{F}(\text{p},\gamma)^{19}\text{Ne}$ reaction.

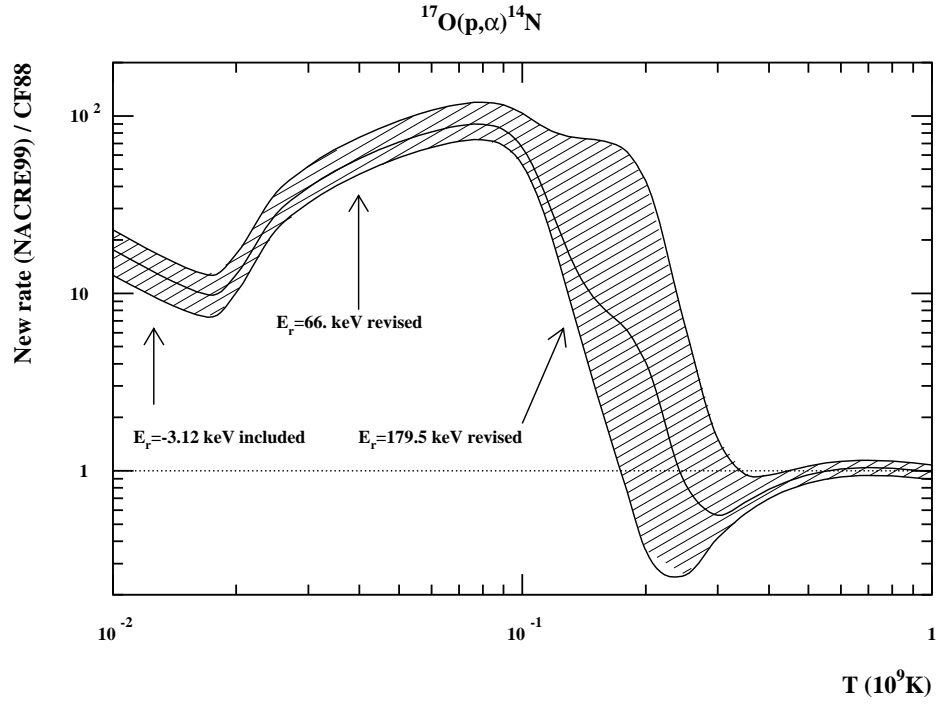


Fig. 8. Comparison between NACRE (low, recommended and high) and CF88 rates for the $^{17}\text{O}(\text{p},\alpha)^{14}\text{N}$ reaction. The origins for the differences are labeled with the energy of the corresponding resonances. (See Angulo et al. 1999 for more detail.)

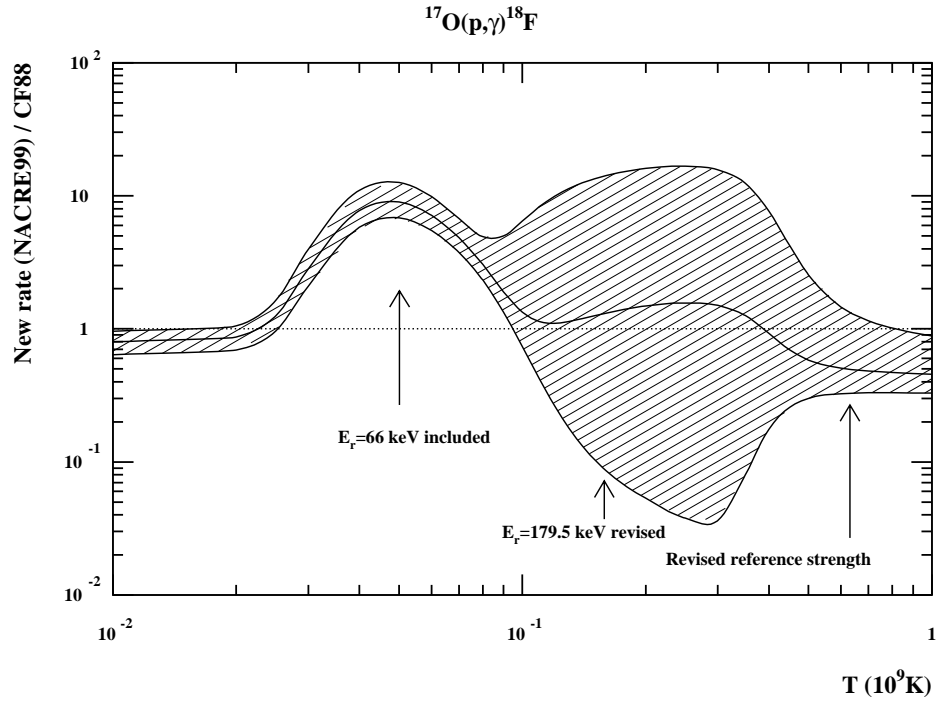


Fig. 9. Same as Fig. 8 but for the $^{17}\text{O}(\text{p},\gamma)^{18}\text{F}$ reaction.

Table 2. $^{18}\text{F}(\text{p},\gamma)^{19}\text{Ne}$ and $^{18}\text{F}(\text{p},\alpha)^{15}\text{O}$ rates

T (10 ⁹ K)	$^{18}\text{F}(\text{p},\alpha)^{15}\text{O}$			$^{18}\text{F}(\text{p},\gamma)^{19}\text{Ne}$		
	low	nominal	high	low	nominal	high
0.030	0.323E-16	0.841E-13	0.841E-12	0.605E-13	0.302E-09	0.308E-08
0.040	0.555E-14	0.338E-11	0.338E-10	0.108E-10	0.123E-07	0.132E-06
0.050	0.215E-12	0.445E-10	0.444E-09	0.431E-09	0.165E-06	0.197E-05
0.060	0.352E-11	0.349E-09	0.348E-08	0.723E-08	0.133E-05	0.180E-04
0.070	0.328E-10	0.195E-08	0.194E-07	0.689E-07	0.765E-05	0.116E-03
0.080	0.208E-09	0.843E-08	0.835E-07	0.444E-06	0.339E-04	0.568E-03
0.090	0.991E-09	0.296E-07	0.292E-06	0.216E-05	0.122E-03	0.221E-02
0.100	0.383E-08	0.883E-07	0.865E-06	0.843E-05	0.372E-03	0.717E-02
0.110	0.126E-07	0.231E-06	0.225E-05	0.279E-04	0.990E-03	0.201E-01
0.120	0.367E-07	0.544E-06	0.523E-05	0.810E-04	0.237E-02	0.502E-01
0.130	0.992E-07	0.118E-05	0.112E-04	0.212E-03	0.519E-02	0.114E+00
0.140	0.262E-06	0.239E-05	0.222E-04	0.516E-03	0.106E-01	0.238E+00
0.150	0.703E-06	0.467E-05	0.416E-04	0.120E-02	0.203E-01	0.464E+00
0.160	0.194E-05	0.899E-05	0.748E-04	0.271E-02	0.372E-01	0.857E+00
0.180	0.145E-04	0.344E-04	0.222E-03	0.135E-01	0.114E+00	0.255E+01
0.200	0.867E-04	0.138E-03	0.618E-03	0.622E-01	0.323E+00	0.657E+01
0.250	0.251E-02	0.291E-02	0.656E-02	0.143E+01	0.339E+01	0.457E+02
0.300	0.237E-01	0.256E-01	0.436E-01	0.129E+02	0.224E+02	0.205E+03
0.350	0.115E+00	0.121E+00	0.182E+00	0.630E+02	0.957E+02	0.669E+03
0.400	0.366E+00	0.383E+00	0.537E+00	0.212E+03	0.302E+03	0.173E+04
0.450	0.887E+00	0.921E+00	0.124E+01	0.577E+03	0.794E+03	0.382E+04
0.500	0.178E+01	0.184E+01	0.242E+01	0.140E+04	0.189E+04	0.758E+04
0.600	0.489E+01	0.504E+01	0.648E+01	0.662E+04	0.879E+04	0.248E+05
0.700	0.990E+01	0.102E+02	0.130E+02	0.240E+05	0.317E+05	0.689E+05
0.800	0.167E+02	0.172E+02	0.220E+02	0.675E+05	0.887E+05	0.165E+06
0.900	0.251E+02	0.258E+02	0.337E+02	0.153E+06	0.201E+06	0.341E+06
1.000	0.349E+02	0.361E+02	0.481E+02	0.295E+06	0.387E+06	0.623E+06
1.250	0.649E+02	0.679E+02	0.982E+02	0.939E+06	0.123E+07	0.189E+07
1.500	0.101E+03	0.107E+03	0.169E+03	0.196E+07	0.258E+07	0.394E+07
1.750	0.140E+03	0.151E+03	0.259E+03	0.321E+07	0.424E+07	0.655E+07
2.000	0.180E+03	0.197E+03	0.361E+03	0.454E+07	0.601E+07	0.948E+07
2.500	0.262E+03	0.292E+03	0.581E+03	0.703E+07	0.936E+07	0.155E+08
3.000	0.347E+03	0.390E+03	0.800E+03	0.897E+07	0.120E+08	0.209E+08